Supplemental Methods and Material

Commercial antibodies used in this study

The used antibodies were purchased as follows: Goat polyclonal anti-APPL1 from Abcam, mouse monoclonal anti-clathrin heavy chain (clone X22) from ABR, mouse monoclonal anti-myosin VI from Sigma, mouse monoclonal anti-GM130 and mouse monoclonal anti-γ-Adaptin and anti SNX1 from BD Transduction Laboratories, goat polyclonal anti-GIPC from Santa-Cruz.

Total internal reflection microscopy

Cells were plated on glass bottom dishes (MatTek Corporation) and TIRF microscopy was achieved using an objective-type set-up with an Olympus IX-70 inverted microscope and 60X, 1.45 NA TIRF microscopy lens. To excite the specimen, 488nm and 568nm light from electronically shuttered Argon and Argon/Krypton lasers (Melles Griot, Carlsbad CA), respectively, were coupled to a single-mode fiber and to the TIRF microscopy condenser (Olympus). The calculated penetration depth (1/e) of the evanescent field was ~100nm. Light passed through a "GFP-RFP-Cy5" triple dichroic filter (Semrock) and images were collected with an iXon 887 EM-CCD camera (512X512, back-illuminated; Andor Technologies). Acquisition was controlled using iQ software (Andor Technologies) and 50-500 msec exposures were acquired at 0.25 - 0. 5 Hz. For rapid confocal imaging, an 'Ultraview 5-line' spinning-disk confocal system (Perkin Elmer) with an IX-71 inverted microscope (Olympus) was used. Samples were excited at 488nm and 568nm, imaged through 60X or 100X (1.4 N.A.) oil objectives and

detected with a 1Kx1K EM-CCD camera (Model C9100, Hamamatsu). Exposure times were 100 - 500msec.

Isothermal Titration Calorimetry (ITC)

Experiments were performed in the Keck Research Facility at Yale University. In each experiment, 3-µl aliquots of peptide solution (2 mM) were injected into a calorimetric cell preloaded with 1.4267 ml of the COOH-terminal region of OCRL (35 µM) using a rotating stirrer syringe (250-µl vol) every 240 s at 30°C. Both the peptide and the protein solution contained 20 mM Hepes, pH 7.0, 20 mM NaCl and were degassed prior to use. To estimate a blank heat effect associated with dilution and mechanical phenomena, peptide injections into degassed buffer were performed before the titration with protein.

Protein crystallization

A GST-selenomethionine-substituted protein, corresponding to the COOH-terminal region (ASH plus Rho-GAP-like domain) of human OCRL1 (residues 564-901), was prepared by growing bacteria in M9 medium supplemented with selenomethionine and with an excess of six amino acids (Thr, Lys, Phe, Le, Ile, Val) to inhibit methionine biosynthesis. The GST tag was removed by PreScission^{TM} protease and the eluted protein was further purified using size exclusion chromatography (Superdex 200) in a buffer containing 20 mM Hepes, 20 mM NaCl, 1 mM DTT, pH7.4. The purified OCRL fragment was concentrated to 8 mg/ml for crystallization. Crystallization conditions were screened using Wizard I and II formulations (Emerald BioStructure) with the hanging drop vapor diffusion method. Crystals were obtained with a 1:1 (v/v) mixture of the

OCRL protein and the mother liquid (100 mM Hepes, pH 7.0, 8.5% PEG 8000, 400 mM NaCl). They appeared in 2-3 days and fully developed in 2-3 weeks at 4^0C. The crystal formed in the space group $P3_221$ with the following unit cell dimensions: a = b = 91.3 Å, c = 103.9 Å, $\alpha = \beta = 90^0$, $\gamma = 120^0$. They contained one molecule per asymmetric unit with 60% solvent.

Crystallographic data collection, structure determination and refinement

Crystals were soaked in cryoprotectant solution by stepwise transfer to well buffer supplemented with 5%, 10%, 15%, 20%, 25% of glycerol, respectively, mounted onto a cryo-loop and flash frozen in liquid nitrogen. SAD oscillation diffraction data were collected at the selenium peak wavelength to d_{min} = 2.8 Å (table I). Diffraction data were processed with HKL 2000 and the structure of the crystal was determined by single anomalous dispersion (SAD) phasing. Five of the six selenium sites were found in anomalous difference Patterson maps calculated using the peak SAD data with CNS. Phasing and density modification were also carried out with CNS. The protein coordinates were refined initially with CNS at 2.8 Å using experimental phases followed by cycles of manual rebuilding with phase combined maps. The structure was ultimately refined against the 2.4 Å refinement data (Supplemental Table 1) by simulated annealing, conjugate gradient minimization, and restrained isotropic B-factor refinement.

Supplemental Figure Legend

Figure S1: APPL1 and rab5 synergize in the recruitment of INPP5B to enlarged endosomes. Cos-7 cells were transfected with constitutive active Rab5 (Myc-rab5Q79L)

together with either RFP-OCRL or RFP-INPP5B and with or without EGFP-APPL1. Expression of Myc-rab5Q79L was detected by immunofluorescence. Double and triple fluorescence images are shown. (Calibration bar=5 μm).

Figure S2:

APPL1 binding requires both the ASH and RhoGAP-like domains of OCRL. Left panel: Fusion proteins used as baits (Ponceau staining) and western blots of the bound material. Right panel: Schematic drawing of the constructs used for the pulldown experiment shown in the left panel. The relative binding of the individual constructs is indicated by + and -.

Figure S3: Sequence alignment of the RhoGAP-like domains of OCRL and INPP5B with the RhoGAP domains of P50RhoGAP and chimaerin. Secondary structure elements are drawn above the alignment. Two mutations found within the OCRL protein in Lowe syndrome patients, I768N and A797P, are labeled by a black triangle. The clathrin box motif and the alternative spliced sequence of OCRL are indicated by a pink and a green bar, respectively. The position of the catalytic arginine residue in *bona fide* RhoGAP domains is boxed. Entrez database accession numbers are as follows: OCRL_Hs, GI: 57209431; Inpp5b_Hs, GI: 59803021; OCRL_Dr, GI: 68374521; Inpp5b_Dm, GI: 54642833; Inpp5b_Ce, GI: 17505597; Inpp5b_Dd, GI: 66828629; P50RhoGAP_Hs, GI: 3660275; Chimaerin_Hs, GI: 56967042. (Hs, *Homo sapiens;* Dr, *Danio rerio;* DM, *Drosophila melanogaster;* CE, *Caenorhabditis elegans;* Dd, *Dictyostelium discoideum*)

Figure S4: The RhoGAP-like domain of OCRL does not contain a typical "arginine finger". Close view of the structure of the RhoGAP-like domain of OCRL (blue) superimposed on the RhoGAP domain of P50RhoGAP (red) (PDB ID: 1AM4). The bound Cdc42 is shown in gold. The position of the typical "arginine finger" is replaced by a glutamine in OCRL.

Figure S5: Clathrin box motif of the RhoGAP-like domain of OCRL. The first alpha helix of the RhoGAP-like domain with the adjacent long loop is shown in green. Amino acids of the clathrin box motif ^{702}LIDLE^{706} are shown as sticks.

Figure S6: Phosphoinositide substrate specificity of purified OCRL and INPP5B as determined by the malachite green assay (green color indicates release of free phosphate into the medium). PI(4,5)P_2 and PI(3,4,5)P_3 are the preferred substrates.

Movie 1: TIRF microscopy movie of a Cos-7 cell co-expressing mRFP-LCa (red) and EGFP-OCRL (green). Images were acquired at 1 frame/4 seconds. Playback speed = 12fps (48 x accelerated). White circles highlight examples of CCPs which receive a burst of OCRL before disappearing.

Movie 2: TIRF microscopy movie of a Cos-7 cell co-expressing EGFP-OCRL (left panel) and mRFP-APPL1 (center panel). Merge is on the right. Images were acquired at 1 frame/4 seconds. Playback speed = 25fps (100 x accelerated).

Movie 3: Detail of the edge of a Cos-7 cell co-expressing EGFP-OCRL (green) and mRFP-APPL1 (red), and imaged by TIRF microscopy. Images were acquired at 1 frame/4 seconds. Playback speed = 10fps (40 x accelerated). White circles highlight examples of structures expressing OCRL and then APPL1 sequentially.

Figure S1

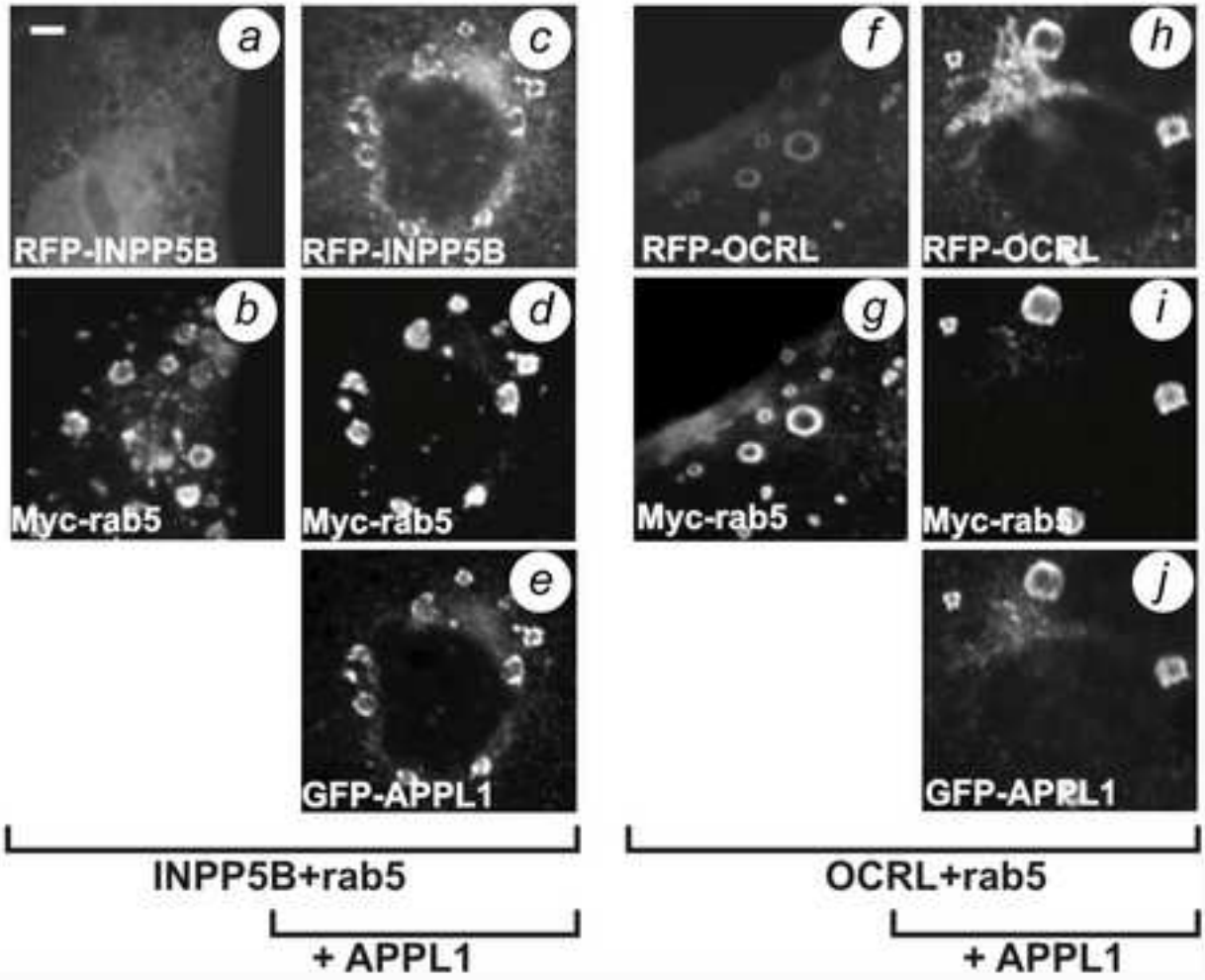

Figure S2

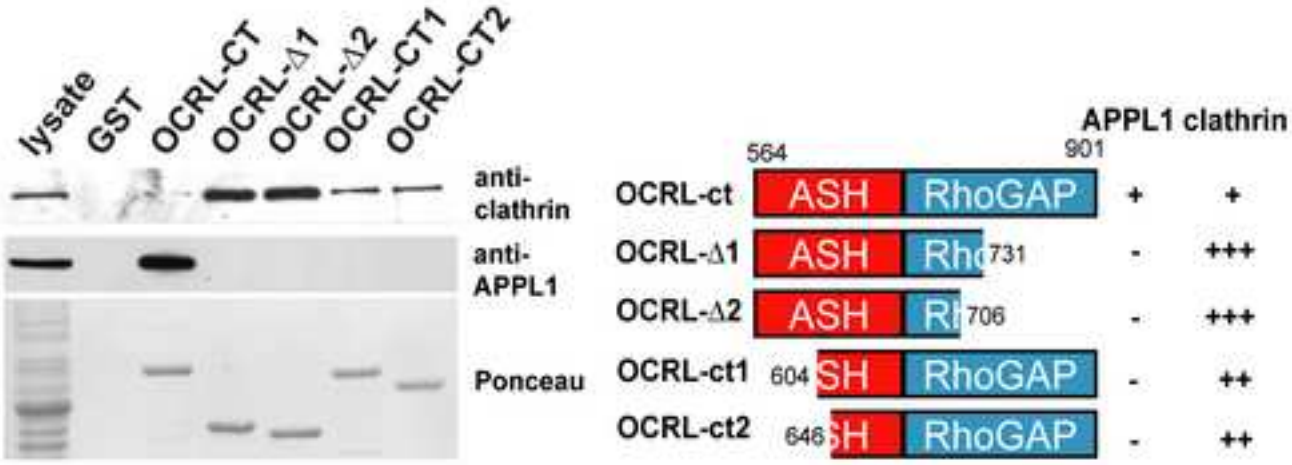

Supplemental Figures and Text

Figure S3

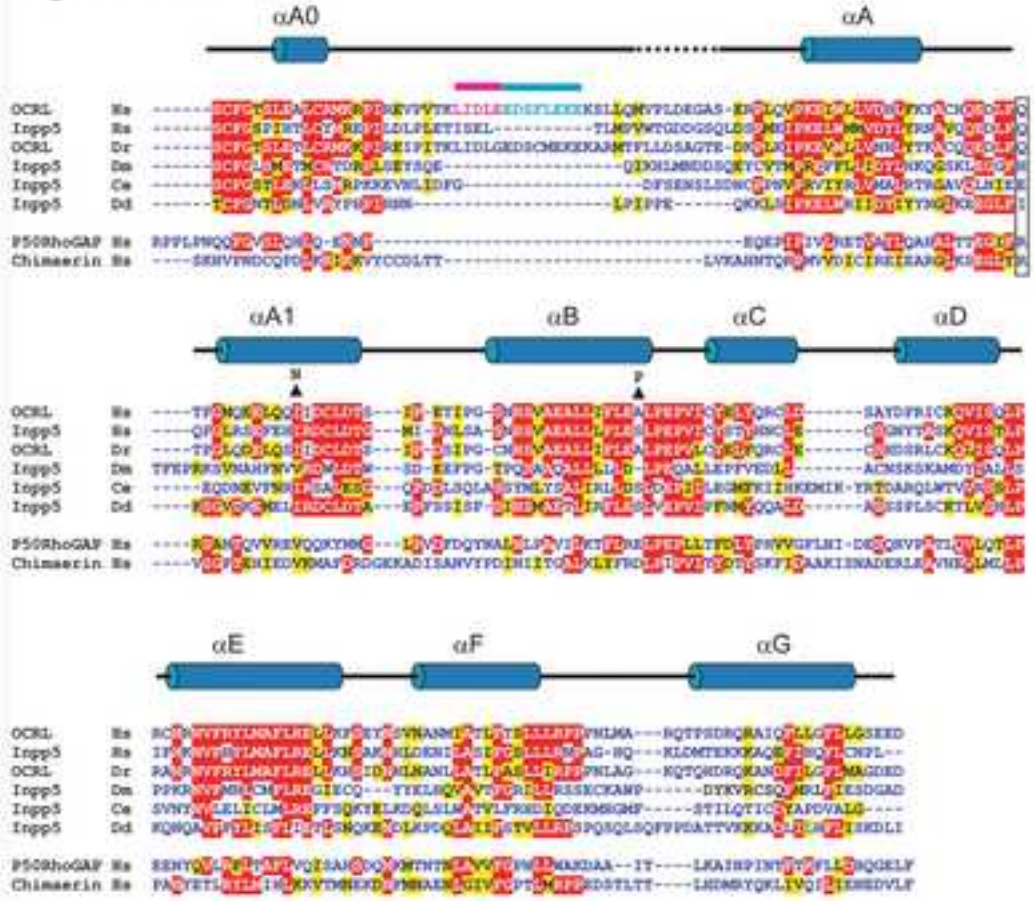

Figure S4

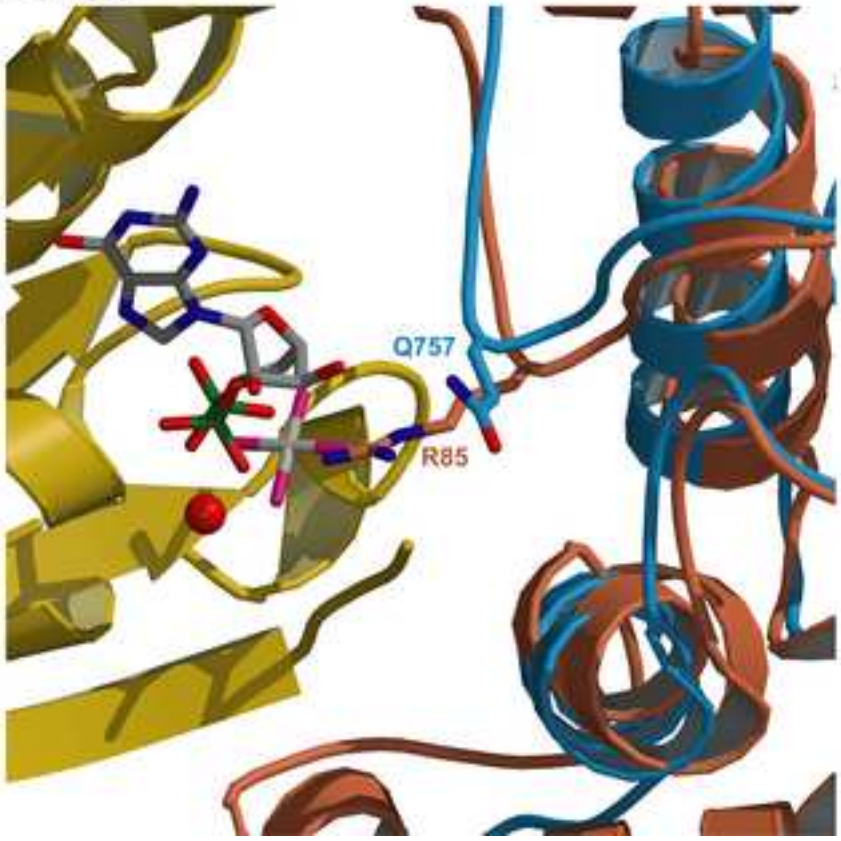

Supplemental Figures and Text

Figure S5

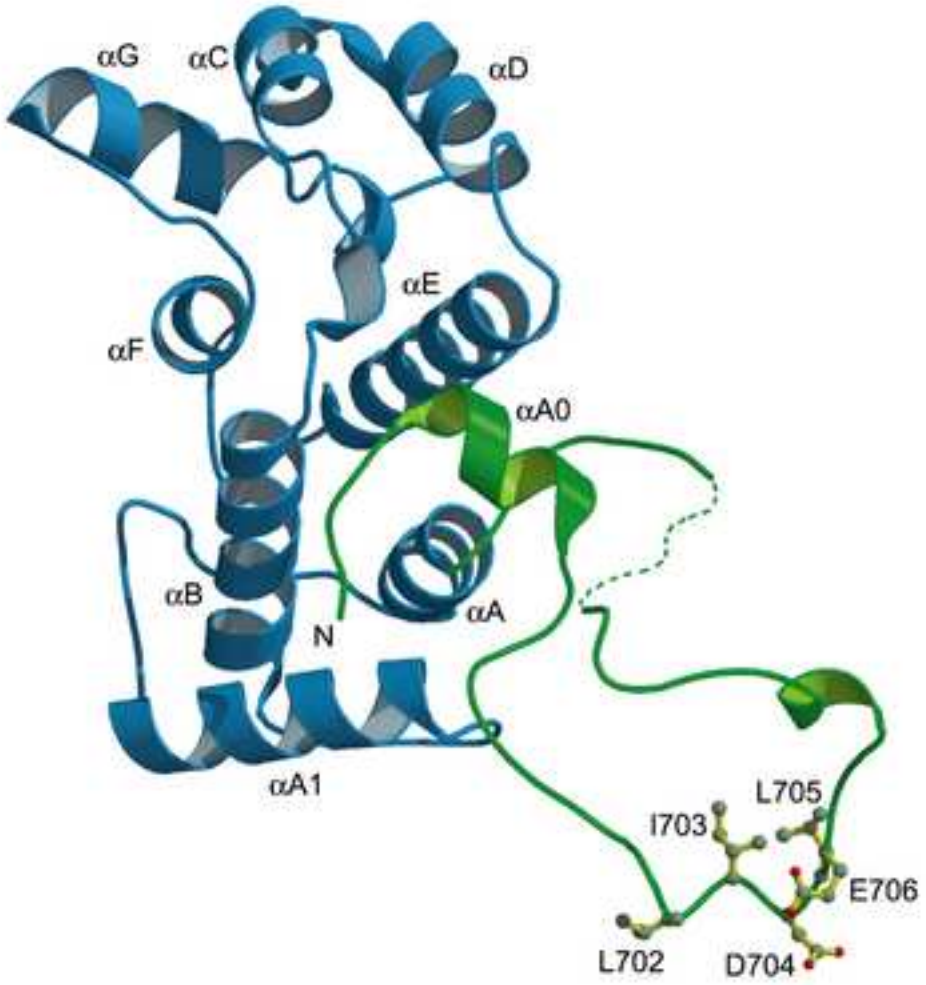

Figure S6

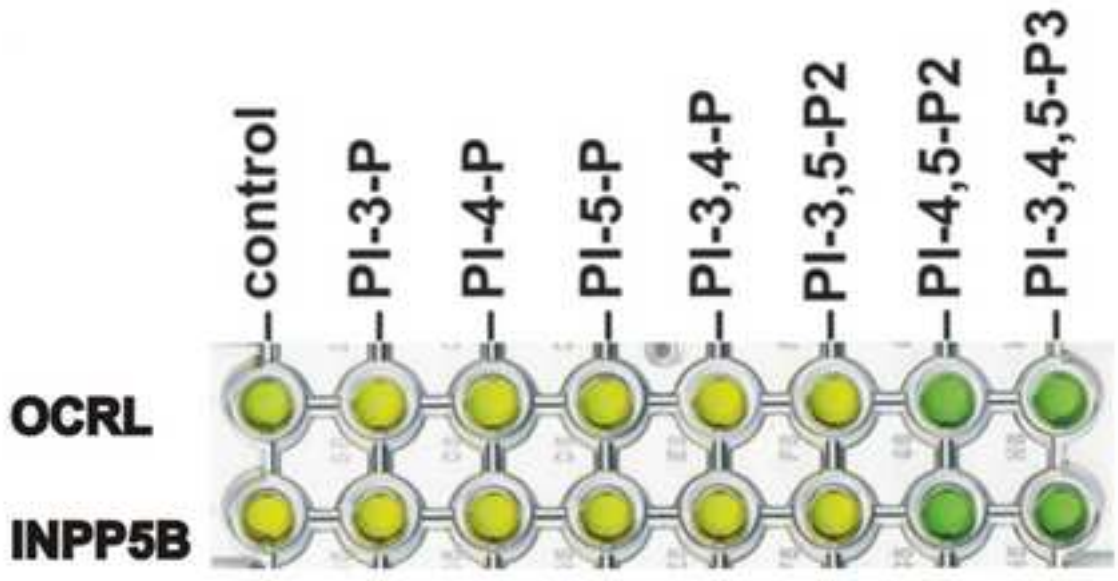

Supplemental Table 1. Data collection, phasing statistics and refinement

A. Data collection and phasing		
Space group	$P3_221$	
Cell dimensions	a = 91.3 Å, b = 91.3 Å, c = 103.9 Å, $\alpha = 90^0$, $\beta = 90^0$, $\gamma = 90^0$	
	SAD phasing data	Refinement data
Wavelength (Å)	0.9793	0.9840
Resolution (Å)	50 – 2.8	50 – 2.4
Unique reflections	23,965	18,866
Multiplicity [a]	10.1(6.7)	11.3(5.6)
Completeness (%)[a]	99.5 (97.8)	92.1 (86.7)
$\langle I \rangle / \langle \sigma \rangle$[a]	51.3(4.9)	43.9(7.5)
R_{sym} [a,b]	0.061(0.293)	0.062(0.258)
Se-SAD FOM	0.21	—
Se-SAD FOMDM	0.91	—
B. Refinement		
Resolution (Å)	50 – 2.4	
R_{crys} / R_{free} (%)[c]	24.8/28.8	
Rms bond length (Å)	0.0073	
Rms bond angles (°)	1.24	
Ramachandran plot		
Most favored/Additional (%)	85.7/14.0	
Generous/Disallowed (%)	0.4/0.0	

[a]Values in parenthesis are for the highest resolution shell.
[b]$R_{sym} = \Sigma_h \Sigma_i |I_I(h) - \langle I(h)| / \Sigma_h \Sigma_i I_I(h)$.
[c]$R_{crys} = \Sigma(|F_{obs}| - k|F_{cal}|) / \Sigma|F_{obs}|$. R_{free} was calculated for 5% of reflections randomly excluded from the refinement.